İSTANBUL TİCARET ÜNİVERSİTESİ
FEN BİLİMLERİ DERGİSİ

Istanbul Commerce University Journal of Science

http://dergipark.org.tr/ticaretfbd

Research Article / Araştırma Makalesi

EVALUATING THE EFFECTS OF THE AUTONOMIC NERVOUS SYSTEM AND SYMPATHETIC ACTIVITY ON EMOTIONAL STATES

OTONOM SİNİR SİSTEMİ VE SEMPATİK AKTİVİTENİN DUYGU DURUMU ÜZERİNDEKİ ETKİLERİNİN DEĞERLENDİRİLMESİ

Fatma PATLAR AKBULUT[1]

https://doi.org/10.55071/ticaretfbd.1125431

Corresponding Author / Sorumlu Yazar
f.patlar@iku.edu.tr

Received / Geliş Tarihi
02.06.2022

Accepted / Kabul Tarihi
23.06.2022

Abstract

Emotion recognition has attracted more interest by being applied in many application areas from different domains such as medical diagnosis, e-commerce, and robotics. This research quantifies the stimulated short-term effect of emotions on the autonomic nervous system and sympathetic activity. The primary purpose of this study is to investigate the responses of 21 adults by attaching a wearable system to measure physiological data such as an electrocardiogram and electrodermal activity in a controlled environment. Cardiovascular effects were evaluated with heart rate variability indices that included HR, HRV triangular-index, rMSSD (ms), pNN5O (%); frequency analysis of the very low frequency (VLF: 0-0,04 Hz), low frequency (LF: 0,04-0,15 Hz), and high frequency (HF: 0,15-0,4 Hz) components; nonlinear analysis. The sympathetic activity was evaluated with time-varying and time-invariant spectral analysis results of the EDA. The participants who experience calmness had a 4,8% lower heart rate (75,06±16,76 and 78,72±16,52) observed compared to happiness. Negative valance with high-arousal emotions like anger was invariably responded to with a peak in skin conductance level. Besides, negative valance with low-arousal emotions like sadness was allied with a drop in conductance level. Anger, in addition to being the most well-known emotion, elicited coherent time-varying spectral responses.

Keywords: Biomedical signal processing, emotion recognition, HRV analysis, spectral analysis.

Öz

Duygu tanıma, tıbbi teşhis, e-ticaret, robotik gibi farklı alanlarda birçok uygulama şekli ile gerçeklenerek yüksek ilgi görmüştür. Bu araştırma, duyguların otonom sinir sistemi ve sempatik aktivite üzerindeki uyarılmış kısa vadeli etkisini ölçmektedir. Çalışmanın birincil amacı, kontrollü bir ortamda elektrokardiyogram ve elektrodermal aktivite vb. fizyolojik verileri ölçmek için giyilebilir bir sistem kullanan 21 yetişkin katılımcının tepkilerini araştırmaktır. Kardiyovasküler etkiler, HR, HRV üçgen-indeksi, rMSSD (ms), pNN5O (%); çok düşük frekans (VLF: 0-0,04 Hz), düşük frekans (LF: 0,04-0,15 Hz) ve yüksek frekans (HF: 0,15-0,4 Hz) bileşenlerinin frekans analizi; SD1, SD2 ve SD oranının doğrusal olmayan analizi, sempatik aktivite, EDA'nın zamanla değişen ve zamanla değişmeyen spektral analiz sonuçları ile değerlendirildi. Sakinlik hisseden katılımcıların mutluluğa kıyasla %4,8% daha düşük kalp atış hızına (75,06±16,76 ve 78,72±16,52) sahip olduğu gözlemlendi. Öfke gibi yüksek uyarılma seviyesi sahip olumsuz duygularda her zaman cilt iletkenlik değerleri zirve ölçümleri tespit ettik. Ayrıca, üzüntü gibi düşük uyarılma düzeyindeki negatif duygulara sahip olanlar iletkenlik seviyesindeki bir azalma ile bağlantılıydı. Öfke, en iyi tespit edilebilen duygu olmasının yanı sıra, zamanla değişen tutarlı spektral tepkiler ortaya çıkardığı görüldü.

Anahtar Kelimeler: Biyomedikal sinyal işleme, duygu tanıma, HRV analizi, spektral analiz.

[1]İstanbul Kültür University, Faculty of Engineering, Department of Computer Engineering, İstanbul, Türkiye.
f.patlar@iku.edu.tr, Orcid.org/ 0000-0002-9689-7486.

1. INTRODUCTION

Emotion recognition is used in many domains today (Dzedzickis et al., 2020). Understanding human emotions is a key factor in a more effective human-computer interaction. Today, the use of this knowledge in the collaborative work of robotic systems in manufacturing increases productivity. Similarly, the emotional states of the customers in the marketing domain are used to reach the sales capacity of the products or services. In educational sciences, it can be ensured that learning processes are improved and perception is strengthened. And in the entertainment industry, emotional state is a strong criterion used to determine the target audience. Therefore, research projects are carried out both in academia and industry to solve this problem.

Since determining the boundaries between emotion, emotion, mood, and affect keywords is a challenging process, innovative approaches are required. Emotion recognition clues which is a key component of affective computing can be extracted from facial expressions, bio-markers, voice, and text by using the opportunities provided by developing sensors and communication technologies (Zhang et al., 2020). Machine learning is considered as one of the most preferred methods for processing and using the collected fusion data. However, the data must be pre-processed before feeding the developed models. Since each biosignal has different characteristics, these multidisciplinary studies also have a signal processing pillar. Heart Rate Variability (HRV), Electroencephalography (EEG), Electrodermal Activity (EDA), temperature, and respiration patterns are mostly used.

Studies have shown that heart rate variability is a serious metric in a variety of other physiological, psychological and psychosocial conditions, other than direct heart disease, from depression to anxiety, stress, and panic (Klein et al. , 1995; Kawachi et al., 1995; Balogh et al., 1993). Moreover, it is seen that HRV changes according to psychosocial factors. Many studies suggest a link between negative emotions and decreased HRV. Also, lower HRV was observed in anxious and depressed individuals (Gorman & Sloan, 2000). The motive is that both the sympathetic and parasympathetic branches of the autonomic nervous system are involved in the regulation of heart rate (HR). Sympathetic nervous system (SNS) activity decreases HRV while increasing HR, and parasympathetic nervous system (PNS) activity decreases HRV while decreasing HR (Berntson et al., 1997). The contributions of this paper are two-fold:

- Distinguishing emotions with time invariant and time variant approaches
- Modeling emotion using multiple bio-signals

The next sections are structured as follows. Section II reviews emotion recognition studies through HRV analysis in the literature. Section III describes and details the detection of autonomic nervous system activity with HRV analysis and how sensor data is processed. Section IV depicts the results and finally, Section V summarizes the main findings and concludes the paper.

2. RELATED WORK

As the evidence shows that positive emotions elicit different HR, blood pressure, and peripheral vascular resistance responses compared to negative emotions, there is a link between emotional states and autonomic nervous system responses. Hereafter, emotion recognition studies using HRV and sympathetic activity in the literature were surveyed. In the study (Takeshita et al., 2021), in which smart watches were used for HRV measurement, 10 participants were asked to watch a 10-minute horror movie. During the experiments, 11 different features were extracted from the frequency and time domain, and a machine learning model was developed to separate the participants from Fear and Fear- lessness Situations. It has been reported that the Support Vector Machine-based model works with 5-Fold-cross-validation achieved more than 90% accuracy. The

scope of this study is limited only to horror movies, but in future work, comedies, emotional movies, and romantic movies are targeted. Cosoli et. al (2021) investigated emotion recognition by HRV analysis on PPG signals. This article aimed to enhance the performance of emotion recognition by considering PPG signals during vocal stimulation. In doing so, it employed a new data artifact correction method and a Support Vector Machine (SVM) classifier. Researchers have observed that the utilization of electrodermal activity (EDA) in addition to the use of PPG signal as the main source increases the accuracy of the classifier.

In another study (Singson et al., 2021) using deep learning powered by ResNet architecture, the developed CNN model distinguished happy, sad, neutral, fear, and anger emotions from collected data fusion. The CNN classifier was fed with facial expressions and ECG signals of participants. A wearable sensor system based on Arduino Uno microcontroller was also developed to measure the ECG signals and transfer them instantly to the machine learning model. In experiments based on 13 different observations using the proposed model, 68,42% accuracy was achieved. In the study Adha & Igasaki (2020) conducted to determine the 3 negative emotions, drowsiness, stress, and tiredness, in the domain of driving, 120 minutes of simulator driving was performed. RR peaks were extracted from the ECG signal using the Pan–Tompkins algorithm and generated as the primary feature. In addition, blood pressure and salivary amylase were recorded. In experiments conducted over 20 driving sessions, the magnitude of the regression coefficient was calculated for all three emotions and it was observed that the values varied between 4,20 and 5,74.

Emotion recognition is also used in the diagnosis of psycho-neural diseases. Yamuza et al. (2019) proposed a model that supports HRV analysis with respiration, unlike other studies. Five emotional states, relax, joy, fear, sadness, and anger, were distinguished within the scope of the study, and the HRV and respiration spectra were mostly seen between relax and joy, negative valance and joy, and fear and sadness. As the primary output of the research is; the use of the correlation between HRV and respiration in emotion recognition applications is promising. In the study Barrett & Popovi (2015) investigating the effect of positive emotions on workplace performance, it was aimed to reveal the changes on the autonomic nervous system with HRV. This survey paper focused on the reflection of psychological level changes on emotions. It was concluded that positive mood states positively reflect on workplace performance and strengthen the ability to cope with challenging situations. Yu and Chen's research (2015) targeted optimization of feature selection by genetic algorithm. The Input was obtained from 4 different perspectives: time-domain, frequency-domain, Poincare plot, and differential features of HRV analysis. Before the emotion recognition using the SVM classifier, the genetic algorithm was employed for the feature selection process, acting as dimension reduction and dramatically affecting the accuracy.

Another important biosignal is EDA which has lately assembled attention as an alternative for evaluating sympathetic activity because sympathetic nerves only stimulate sweat glands. In addition, to recognizing emotion it is also helpful to detect activities like Posada-Quintero et al. (2018) study. They proposed a spectral analysis approach to assess skin sympathetic nervous activity. They analyzed low and high-intensity exercise and found that sympathetic activity shifts to higher frequencies during intense physical activity. In another study to recognize emotion (Yin et al., 2022), they are proposing a framework via combining EDA features and the evoked music features. Then they compare the effectiveness with DEAP and AMIGOS datasets to validate that the fusion features are a reliable solution for emotion recognition.

In the study of Domínguez-Jiménez et al. (2020) to recognize emotion from physiological signals, the participants' heart rate, and galvanic skin response were measured, and components of frequency and time domains were extracted. Models developed for high accuracy recognition of three emotions -amusement, sadness, and neutral- through the sympathetic activity were evaluated successfully. Sepúlveda et al. (2021) performed emotion recognition over nonintrusive

physiological signals using ECG recordings from the AMIGOS dataset. The positive effect on the recognition success in the study depends on the extraction of ECG features. Models that recognize emotions of arousal and valance planes with high accuracy are designed for wearable systems especially to be used in HCI problems. Emotion recognition is of critical importance for many domains by being handled from different perspectives. The prominent common point of the studies is user addiction. A user-independent emotion recognition model was proposed in the study of Albraikan et al. (2018) It is designed to identify the fusion sensor data in an ensemble structure. Models that can recognize valence and arousal emotions with an accuracy of over 93% have been developed.

When the selected studies are inspected, we observed that the studies vary between target emotion analysis and generic recognition. We have seen that some studies are specifically geared towards recognizing emotions rather than working generically. These studies aiming at recognizing specific emotions were found to be more accurate. One of the main characteristics in which the studies differed was user dependency. Since user dependent systems would be more difficult to service, their use was not found practical. In addition, while HRV was used as the main input, the supporting data such as facial expressions etc. increased the recognition accuracy.

3. MATERIALS AND METHODS

3.1. Data Collection

Subjects were 21 adults (12 men, 9 women; the median age of 27 yr.). There were no significant differences in the total sample between the participants, health status, age, or sex. During the emotion elicitation experiment, two biosignals: ECG and EDA were gathered via a wearable sensor. The system recorded data with a sample rate of 250 Hz. Three lead electrodes were located in the Einthoven triangle position for the ECG data acquisition. EDA sensors were located on the second and third fingers of the left hand.

3.2. Processing of Sensor Data

Ambulatory ECG signals are often contaminated by physiological and environmental artifacts such as skin-electrode interface, movement, respiration, muscle contraction, baseline drift, and power line interference which contain frequency components. Baseline wander owing to respiration comprises low-frequency components (0-0,5 Hz); muscle contraction contains high frequencies (50-60 Hz) and power line interference too, and motion artifacts largely yield high amplitude sharp waves. Motion artifact is commonly further obscure of noise to be eliminated from ECG since its spectrum entirely overlaps, and its morphology usually look-alike that of the P, QRS, and T waves.

We reduced the noise in three steps. The first step in reducing low-frequency baseline wander is established on discrete wavelet transformation (DWT), and the second step reduces high-frequency components with Empirical Bayes posterior wavelet via individual adaptive threshold. As the last step, since corrupted ECG heartbeats affect the results of analysis completely outliers that were considered abnormally deviating from adjacent segments were removed by calculating the deviations of the data (Figure 1).

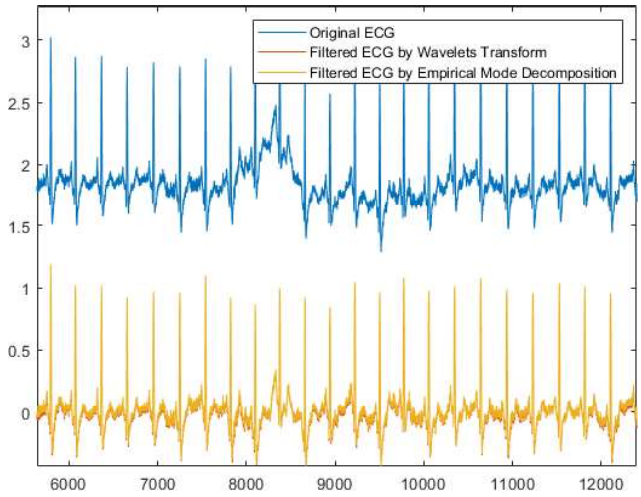

Figure 1. Sample of ECG Signal with Baseline Wander and Filtered ECG

Following the noise reduction, a mixed model has been employed that contains Pan & Tompkins (Pan & Tompkins, 1985) algorithm and rule-based peak detection to detect the RR intervals by linear filtering, nonlinear transformation, and rule-based techniques. Approximate entropy was calculated to determine the complexity and noise level before analyzing the signal. Accordingly, the value of the signal, whose noise is reduced, has been calculated on average 55 which over 100 points indicate that the noise level and regularity of the signal are normal (Pincus, 1995).

3.3. Detection of Autonomic Nervous System Activity

A heart Rate Variability (HRV) analysis was achieved to distinguish features of the ECG signal. During HRV analysis, standard measurements were evaluated with time and frequency domain and components of nonlinear methods.

In the time domain analysis, the intervals between sequential normal complexes at any point in time are determined. For this purpose, heart rate is determined by detecting RR intervals in order to capture instant changes of heart rate in the ECG records. Time-domain measurements included the calculations of the instant statistical indexes derived from the differences between the RR intervals over 1-minute period during watching. During the analysis, first we calculated $rMSSD = \sqrt{\frac{1}{n-1}\sum_{i=1}^{n-1}(RR_{i+1} - RR_i)^2}$ from the root mean square of consecutive differences to display the short-term variability. Also, $NN50 = P(|RR_{i+1} - RR_i| > 50ms)$ was calculated, consecutive RR intervals differences which is higher than 50 ms are taken corresponding relative amount $pNN50 = \frac{NN50}{(n-1)} \times 100$, by dividing the total number of RR intervals. Along with that, $HRVTI = \frac{n}{D(X)max}$ triangular index is calculated dividing by total number of interval (n) by height of the density distribution $(D(X)max)$.

Also to evaluate the correlation between consecutive RR a nonlinear method the Poincaré plot (Figure 1) was used. Each RR_i is shown with a graph drawn against the next RR_(i+1) range.

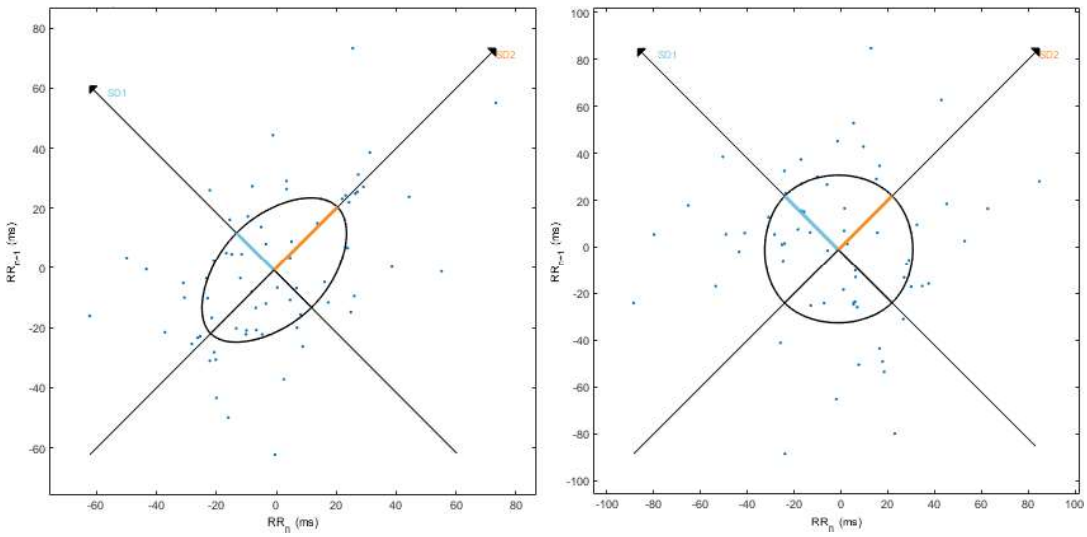

Figure 2. Positive and Negative Valance of Poincare

SD1 variable representing long-term records that reflects HRV and wide variability. SD2 presents the variability of pulse and parasympathetic activity. $SD1/SD2 = \frac{\sqrt{\frac{1}{2}\sigma\,(RR_{i+1}-RR_i)}}{\sqrt{\frac{1}{2}\sigma\,(RR_{i+1}+RR_i)}}$ show the ratio between the short and long variations of the RR intervals.

During the frequency domain analysis, the power spectrum parameters were calculated by the Fourier Transform and an autoregressive (AR) model. The power accommodated in the low- and high-frequency bands ($LF = \int_{0,04}^{0,15} f(\lambda)\, d\lambda$ and $HF = \int_{0,15}^{0,40} f(\lambda)\, d\lambda$), and the LF:HF ratio are calculated to reflect the balance of sympathetic and parasympathetic modulation are calculated over the 1-min monitoring period for each emotion. In the heart rate power spectrum analysis, we followed the following procedures; (i) finding the RR interval, (ii) defining an instantaneous HR with low threshold filtering, and (iii) estimating the spectral features of the signal (Figure 3). We computed a power spectrum for frequencies above 0,01 Hz from a 1-min segment of consecutive peaks that represent heart rates.

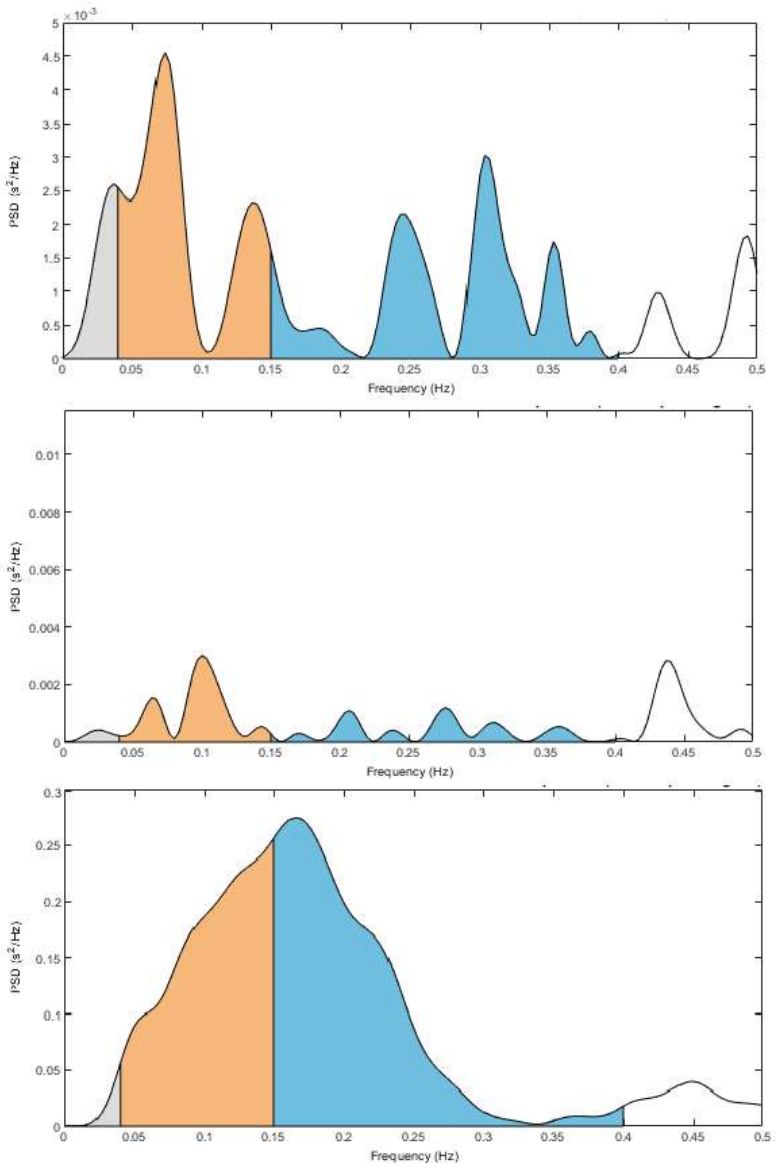

Figure 3. FFT Spectrum of A High Arousal Emotion (Fear - HR: bpm) and Low Arousal Emotion (Calmness - HR: 65 bpm and Sadness - HR: bpm) of RR Series

Heart rates and their accompanying heart rate power spectrum values are shown in Figure 3. Readers note that the three groups of peaks, the largest group at the respiratory high frequency (HF) near 0,2 Hz and the other group at lower frequencies (LF) placed between 0,15 and 0,05 Hz, and the smallest group of peaks at very low frequencies (VLF) in 0 and 0,04.

3.4. Estimation of Sympathetic Activity

As the primary step, the first derivative of the clean EDA signal was calculated. In the process of determining the onset of the skin response, we aimed to find the moment when the rapid falls below the minimum speed. We only evaluated the rise of each event, because the basic idea was to count the spontaneous rise and fall in a longer recording and to obtain their amplitude. The half-life period of the skin reaction is provided by the descending wave as additional info. We used a low-pass filtered EDA to detect skin reactions and smoothed the raw EDA without affecting the initial slope of the larger increments. When examining EDA data, one of the most important points should be to decide whether overlapping increments should be counted independently and brought

together as an event. If the sequential event occurred in less than 700ms, we combined it with the previous event.

Following that, the time-variant and time-invariant spectral analyses have been employed on measured signals. In order to examine the changes in the frequency distribution of our signal, we used the maximum frequency (Quintero et al., 2018) to define the upper-frequency limit of the EDA signal. The criterion for defining maximum frequency is to find a frequency at which the integration of the spectral power from it to the Nyquist frequency is less than 5% of the total power. The maximum frequency is computed and averaged over the five-minute periods of EDA signal to detect the periodicities in the data by learning the amount of power contained in a spectral band, the time-invariant power spectra of the signal were measured by applying Welch's periodogram with 33% overlap. For each segment, a 64 points length Hanning window was applied, for each windowed Fast Fourier Transform (FFT) was computed, and the power spectra of the signal segments were averaged. This technique provides precise amplitude approximations and one of the highest time-frequency resolutions (Boashash, 2015) by utilizing variable frequency complex demodulation which is shown in Figure 5. We calculated the spectral estimation for each time point of the time-frequency representation to compute maximum frequencies. During the process, we computed the spectrogram over the 0,045 - 4 Hz band and discard content below the −60 dB power level to depict only the main frequency components. We used 0% overlap to spot the tone durations and their locations in time.

4. EXPERIMENTAL RESULTS

This section presents the main findings of the study, which includes a widespread description of the biosignals gathered during the emotion elicitation experiments, their main characteristics, and parameters calculated using FFT, AR, and time-varying and time-invariant spectrum analysis performed to evaluate the significance of the results.

Table 1 shows time domain results of HRV with standard error for anger, calmness, disgust, fear, happiness and sadness. We measured Mean RR (ms), STD RR (ms), Min HR (bpm), Mean HR (bpm), Max HR (bpm), STD HR (bpm), RMSSD (ms), NN50 (beats), pNN50 (%), RRtri and TINN (ms) to characterize emotions. Mean RR max value (801,43) is observed for anger and the min value (786,15) is observed for happiness. The highest values for STD HR, RMSSD, RRtri and TINN were observed in anger as 23,42, 86,53, 8,67 and 279,85, respectively. The emotion of happiness had the lowest values in STD HR (8,14), NN50 (23,23), and pNN50 (27,16), while it had the highest values for Min HR (72,13) and Mean HR (78,72). According to Table 1, sadness, another prominent emotion, showed the lowest values in STD RR (54,43), Max HR (87,80), RMSSD (75,38), RRtri (7,57) and TINN (205,38). We also found that the highest measurements of the emotion of fear were made for 3 values, 91.567 for Max HR, 26,19 for NN50 and 30,94 for pNN50. No markers were detected for calmness and disgust.

From the RR intervals originating from the 1-minute segment, power spectral analyses of each successive data point were performed in a sequential mode with the use of FFT and AR methods. A fixed re-sampling frequency per 1-minute period was used. Tables 2 and 3 show the FFT and AR spectrum results for VLF (Hz), LF (Hz), HF (Hz), VLF (ms2), LF (ms2), HF (ms2), VLF (log), LF (log), HF (log), VLF (%), LF (%), HF (%), LF (n.u.), HF (n.u.), TP (ms2) and LF/HF. We found that the FFT spectrum results are more indicative in the identification of emotions, compared with AR spectrum results.

Table 1. Time Domain Results of HRV with Standard Error

	Mean RR (ms)	**STD RR (ms)**	**Min HR (bpm)**	**Mean HR (bpm)**	**Max HR (bpm)**	**STD HR (bpm)**	**RMSSD (ms)**	**NN50 (beats)**	**pNN50 (%)**	**RRtri**	**TINN (ms)**
anger	**801,43± 132,91**	**66,98± 54,02**	**68,95± 12,37**	77,53± 16,74	89,69± 25,97	**23,42± 103,20**	**86,53± 86,67**	25,38± 28,52	30,03± 26,38	**8,67± 4,27**	**279,85± 210,73**
calmness	794,38± 129,12	61,90± 55,48	69,95± 13,38	75,06± 16,76	89,32± 26,84	8,58± 12,60	81,19± 90,25	23,58± 28,41	27,53± 25,28	8,31± 3,65	246,12± 174,75
disgust	799,61± 125,29	59,38± 54,13	70,00± 11,51	**77,31± 15,11**	88,33± 29,35	8,63± 16,40	82,58± 87,91	24,48± 25,15	30,24± 26,13	8,402± 4,71	247,83± 207,18
fear	799,95± 135,81	63,54± 52,36	70,48± 14,30	77,93± 18,24	**91,567± 32,15**	11,13± 25,97	84,88± 85,84	**26,19± 29,63**	**30,94± 26,29**	8,38± 3,80	263,63± 201,84
happiness	**786,15± 122,21**	57,05± 50,47	**72,13± 13,82**	**78,72± 16,52**	90,09± 25,70	**8,14± 11,91**	76,02± 84,56	**23,23± 27,88**	**27,16± 25,65**	8,20± 3,86	232,12± 175,35
sadness	799,60± 132,02	**54,43± 51,08**	71,18± 11,79	77,54± 15,94	**87,80± 23,76**	8,36± 15,47	**75,38± 82,43**	24,62± 27,77	29,440± 26,38	**7,57± 3,62**	205,38± 149,37

Table 2. FFT Spectrum Results of HRV with Standard Error

	VLF (Hz)	**LF (Hz)**	**HF (Hz)**	**VLF (ms^2)**	**LF (ms^2)**	**HF (ms^2)**	**VLF (log)**	**LF (log)**	**HF (log)**	**VLF (%)**	**LF (%)**	**HF (%)**	**LF (n.u.)**	**HF (n.u.)**	**TP (ms^2)**	**LF/HF**
anger	0,04± 0,00	0,09± 0,00	0,27± 0,01	252,57± 59,18	2172,62± 611,22	3362,07± 1075,19	4,27± 0,24	6,37± 0,25	6,47± 0,26	7,68± 0,98	43,40± 2,63	48,77± 3,00	47,71± 3,01	52,13± 3,00	5794,04± 1677,72	1,66± 0,34
calmness	0,04± 0,00	0,09± 0,00	0,27± 0,01	141,79± 28,41	1476,39± 334,30	2588,25± 720,23	3,88± 0,24	6,19± 0,25	6,45± 0,25	5,49± 0,67	43,23± 2,91	51,14± 3,18	46,23± 3,17	53,63± 3,16	4209,74± 969,98	1,47± 0,28
disgust	0,04± 0,00	0,09± 0,01	0,29± 0,01	112,91± 34,84	1164,94± 293,01	2583,91± 672,71	3,45± 0,24	5,78± 0,26	6,22± 0,26	5,50± 0,87	38,95± 3,10	55,29± 3,43	41,91± 3,40	57,81± 3,38	3872,19± 954,31	1,33± 0,23
fear	0,04± 0,00	0,08± 0,00	0,29± 0,01	154,78± 31,99	1738,48± 541,26	2607,27± 768,15	4,03± 0,22	6,16± 0,22	6,40± 0,25	6,28± 0,74	42,00± 3,06	51,46± 3,07	44,86± 3,21	54,86± 3,19	4506,87± 1270,99	1,38± 0,21
happiness	0,03± 0,00	0,09± 0,00	0,30± 0,01	71,99± 31,99	1160,34± 541,26	1925,54± 768,15	3,32± 0,22	5,81± 0,22	5,98± 0,25	5,30± 0,74	44,85± 3,06	49,63± 3,07	47,83± 3,21	51,94± 3,19	3163,34± 1270,99	1,87± 0,21
sadness	0,03± 0,00	0,10± 0,00	0,31± 0,01	66,79± 19,26	747,10± 158,45	1899,44± 507,99	3,20± 0,20	5,58± 0,23	6,08± 0,25	4,50± 0,57	37,94± 2,96	57,27± 3,03	39,86± 3,12	59,83± 3,09	2722,39± 648,68	1,27± 0,31

Table 3. AR Spectrum Results of HRV with Standard Error

	VLF (Hz)	LF (Hz)	HF (Hz)	VLF (ms^2)	LF (ms^2)	HF (ms^2)	VLF (log)	LF (log)	HF (log)	VLF (%)	LF (%)	HF (%)	LF (n.u.)	HF (n.u.)	TP (ms^2)	LF/HF
anger	0,03±0,00	0,10± 0,00	0,26± 0,01	284,60± 58,61	1673,08± 372,40	3647,78± 1132,27	4,67± 0,22	6,34± 0,24	6,68± 0,26	7,35± 0,57	39,59± 2,93	52,91± 3,23	43,31± 3,31	56,53± 3,29	5614,36± 1504,24	1,47± 0,31
calmness	0,04± 0,00	0,10± 0,00	0,27± 0,01	178,94± 34,60	1199,76± 264,68	2641,60± 755,92	4,32± 0,22	6,09± 0,25	6,36± 0,26	7,11± 0,51	41,35± 2,74	51,38± 3,00	44,96± 3,05	54,86± 3,03	4027,22± 997,15	1,35± 0,25
disgust	0,04± 0,00	0,11± 0,00	0,30± 0,01	173,24± 38,10	1094,74± 268,54	2669,75± 701,30	4,09± 0,22	5,92± 0,23	6,41± 0,25	6,51± 0,68	37,37± 2,82	55,91± 3,23	40,74± 3,20	59,04± 3,18	3945,89± 952,61	1,10± 0,17
fear	0,03± 0,00	0,10± 0,00	0,28± 0,01	207,88± 39,04	1394,71± 327,74	2298,68± 571,87	4,45± 0,20	6,17± 0,22	6,46± 0,24	7,25± 0,62	40,79± 2,99	51,76± 3,17	44,35± 3,27	55,45± 3,26	3906,99± 885,26	1,39± 0,22
happiness	0,04± 0,00	0,11± 0,00	0,29± 0,01	136,30± 39,04	1028,91± 327,74	2263,36± 571,87	4,07± 0,20	5,93± 0,22	6,17± 0,24	6,83± 0,62	42,27± 2,99	50,68± 3,17	45,87± 3,27	53,89± 3,26	3434,15± 885,26	1,88± 0,22
sadness	0,04± 0,00	0,11± 0,00	0,30± 0,01	106,96± 23,47	769,62± 167,58	1788,17± 466,71	3,84± 0,19	5,72± 0,22	6,15± 0,23	6,12± 0,51	38,54± 2,57	55,07± 2,74	41,33± 2,79	58,38± 2,77	2672,65± 625,12	1,02± 0,14

Quantitative analysis of the shape of the consecutive RR interval of ECS was executed using the nonlinear method of the Poincaŕe plot during the emotion recognition experiment. The markings of the plot were converged around a line with slope = 1 of unitary slope passing through the origin. As the geometry domain of the HRV analysis, Table 4 shows the SD1 (ms), SD2 (ms), and SD2/SD1 ratios of six emotions. SD1 is considered similar to the time-domain analysis parameter RMSSD of short-term HRV. We also used SD2 to reveal the relationship of Low Frequency ms2. Ans finally SD2 and SD1 ratio is computed. We observed a correlation between LF ms2 and SD2 as anger and fear increase in SD2, their values decrease in LF ms2. Similarly, HF is highly associated with anger and fear-based SD2. According to the SD1/SD2 ratio, the lowest value was observed in sadness, while the values in LF ms2 and HF ms2 were lower compared to other emotions. Since the relationship between the frequency domain parameters SD2 and Low Frequency (LF) is used to express sympathetic activity, we found evidence of an almost twofold increase in the relationship between SD2 and High Frequency (HF), so SD2 can be used as an indicator of sympathetic activity.

Table 4. Geometric Domain Results of hrv with Standard Error

	SD1 (ms)	**SD2 (ms)**	**SD2/SD1 ratio**
anger	61,57±8,55	68,93±6,93	1,41±0,09
calmness	57,77±8,90	62,73±6,65	1,38±0,08
disgust	59,39±8,82	58,29±6,67	1,24±0,08
fear	60,40±8,47	63,45±6,48	1,36±0,08
happiness	54,10±8,47	56,51±6,48	1,40±0,08
sadness	53,63±8,13	53,17±6,19	1,22±0,07

Time invariant dynamics of the EDA signal, shown in Table 5 for a group of emotions, were found to be quite similar. During the experiments, we observed the frequency of NS.SCRs increased in direct proportion to the intensity of arousal. Even though NS.SCRs have commonly been expressed by counting in the time domain and delivering an index of the number of NS.SCRs per unit time, these fluctuations have been indicated to be an even more discreet index of sympathetic arousal. Although the SC was not significantly different in high to low arousal, time-varying features of low dominance emotions such as fear, anger, and happiness were significantly different compared to high dominance emotions. Employing the time-varying technique, we found more evidence between emotion groups.

Table 5. Time Varying and Invariant Spectral Analysis Results of EDA Signal for Each Emotion

	Time varying (Hz)	**Time invariant (Hz)**	**SC (V)**	**NS-SCRs (count/sec)**
anger	3,32±0,68	1,15±0,02	0,27±0,02	49,17±1,50
calmness	2,17±0,51	1,07±0,01	0,27±0,02	41,23±0,86
disgust	2,46±0,47	1,13±0,06	0,26±0,02	44,98±1,41
fear	2,51±0,41	1,11±0,06	0,27±0,02	43,63±1,77
happiness	2,97±0,54	1,09±0,03	0,25±0,02	45,60±1,41
sadness	2,44±0,64	1,07±0,01	0,27±0,02	41,21±0,89

5. CONCLUSION AND SUGGESTIONS

In this study, we investigated the biosignals to label the autonomic function and sympathetic activity on six emotional states anger, calmness, disgust, fear, happiness, and sadness. We used multiple analyses to characterize the ECG and EDA signal and evaluated it with components of standard measures, time and frequency domain, nonlinear methods, time-varying, and time-invariant spectrum methods. The findings of the study conducted with bio-signals of 21 participants showed that; calmness and disgust are emotions that are difficult to detect compared to others. We found that the most noticeable emotion is to be found as anger and it is associated with a large number of time-domain makers. We confirmed that FFT and AR methods are not as distinctive as time-domain results. Due to the increase in the practice domains of emotion detection, the need for accurate recognition methods increases. In this study, which evaluated the autonomic nervous system and sympathetic activities as an alternative to artificial intelligence and machine learning methods, it was found that four of six main emotions could be determined with bio-signals accurately. As the continuation of this study author plans to employ new techniques such as trigonometric regressive spectral for evaluating the autonomic nervous system in the detection of emotional states. In this study, the emotion recognition service is user-oriented and making it independent from the user increases the usage areas. In addition, by tuning the recognition models as energy efficient, its effectiveness on wearable systems will increase.

Statement of Research and Publication Ethics
Research and publication ethics have complied in this study.

REFERENCES

Adha, M.S. & Igasaki, T. (2020, July, 20-24). *Concurrent model for three negative emotions using heart rate variability in a driving simulator environment*. 42nd Annual International Conference of the IEEE Engineering in Medicine & Biology Society. 718–721.

Albraikan, A., Tobón, D.P. & El Saddik, A. (2018). Toward user-independent emotion recognition using physiological signals. *IEEE Sensors Journal*. 19(19), 8402-8412.

Balogh, S., Fitzpatrick, D.F., Hendricks, S.E. & Paige, S.R. (1993). Increases in heart rate variability with successful treatment in patients with major depressive disorder. *Psychopharmacology Bulletin*. 29(2), 201-206.

Barrett, H. & Popovi, N. (2015). A meta-synthesis on the effects of combining heart rate variability biofeedback and positive emotion on workplace performance. *International Journal of Social Science Studies.* 3(5), 61-68.

Berntson, G.G., Thomas Bigger, J., Eckberg, D.L., Grossman, P., Kaufmann, P.G., et al. (1997). Heart rate variability: Origins, methods, and interpretive caveats. *Psychophysiology*.34 (6), 623–648.

Boashash, B. (2015). Time-frequency signal analysis and processing: A comprehensive reference. *Academic Press*. Cambridge.

Cosoli, G., Poli, A., Scalise, L. & Spinsante, S. (2021, May, 17-20). *Heart rate variability analysis with wearable devices: Influence of artifact correction method on classification accuracy for emotion recognition*. IEEE International Instrumentation and Measurement Technology Conference. Scotland. 1–6.

Domínguez-Jiménez, J.A., Campo-Landines, K.C., Martínez-Santos, J.C., Delahoz, E. J. & Contreras-Ortiz, S.H. (2020). A machine learning model for emotion recognition from physiological signals. *Biomedical Signal Processing and Control*, 55, 1-11.

Dzedzickis, A., Kaklauskas, A. & Bucinskas, V. (2020). Human emotion recog-nition: Review of sensors and methods. *Sensors*, 20(3), 1-40.

Gorman, J.M. & Sloan, R.P. (2000). Heart rate variability in depressive and anxiety disorders. *American Heart Journal*. 140 (4), S77–S83.

Kawachi, I., Sparrow, D., Vokonas, P.S. & Weiss, S.T. (1995). Decreased heart rate variability in men with phobic anxiety (data from the normative aging study). *The American Journal of Cardiology*. 75 (14), 882–885.

Klein, E., Cnaani, E., Harel, T., Braun, S. & Ben-Haim, S.A. (1995). Altered heart rate variability in panic disorder patients. *Biological Psychiatry*. 37(1), 18–24.

Pan, J. & Tompkins, W.J. (1985). A real-time qrs detection algorithm. *IEEE Transactions on Biomedical Engineering*.3,230–236.

Pincus, S. (1995). Approximate entropy (apen) as a complexity measure. *Chaos: An Interdisciplinary Journal of Nonlinear Science*. 5 (1), 110–117.

Posada-Quintero, H. F., Reljin, N., Mills, C., Mills, I., Florian, J. P., VanHeest, J.L. & Chon, K.H. (2018). Time-varying analysis of electrodermal activity during exercise. *PloS One*, 13 (6), 1-12.

Sepúlveda, A., Castillo, F., Palma, C. & Rodriguez-Fernandez, M. (2021). Emotion recognition from ECG signals using wavelet scattering and machine learning. *Applied Sciences*, 11(11), 1-14.

Singson, L.N.B., Sanchez, M.T.U.R. & Villaverde, J.F. (2021, March, 20-21). *Emotion recognition using short-term analysis of heart rate variability and resnet architecture*. 13th International Conference on Computer and Automation Engineering. Australia. 15–18.

Takeshita, R., Shoji, A., Hossain, T., Yokokubo, A. & Lopez, G. (2021, November, 17-19). *Emotion recognition from heart rate variability data of smartwatch while watching a video*. 13th. International Conference on Mobile Computing and Ubiquitous Network. Tokyo. 1–6.

Yamuza, M.T.V., Bolea, J., Orini, M., Laguna, P., Orrite, C., Vallverdu, M. & Bailon, R. (2019). Human emotion characterization by heart rate variability analysis guided by respiration. *IEEE Journal of Biomedical and Health Informatics*, 23 (6), 2446–2454.

Yin, G., Sun, S., Yu, D., Li, D. & Zhang, K. (2022). A multimodal framework for large-scale emotion recognition by fusing music and electrodermal activity signals. ACM *Transactions on Multimedia Computing, Communications, and Applications.* 18(3), 1–23.

Yu, S.N. & Chen, S.F. (2015, August, 25-29). *Emotion state identification based on heart rate variability and genetic algorithm.* 37th Annual International Conference of The IEEE Engineering in Medicine and Biology Society. 538–541.

Zhang, J., Yin, Z., Chen, P. & Nichele, S. (2020). Emotion recognition using multi-modal data and machine learning techniques: A tutorial and review. *Information Fusion*. 59, 103–126.